



Deposited via The University of York.

White Rose Research Online URL for this paper:

<https://eprints.whiterose.ac.uk/id/eprint/114126/>

Version: Accepted Version

Article:

Strong, Samantha L, Silson, Edward H, Gouws, Andre D et al. (2017) Differential Processing of the Direction and Focus of Expansion of Optic Flow Stimuli in areas MST and V3A of the Human Visual Cortex. *Journal of Neurophysiology*. jn.00031.2017. ISSN: 0022-3077

<https://doi.org/10.1152/jn.00031.2017>

Reuse

Items deposited in White Rose Research Online are protected by copyright, with all rights reserved unless indicated otherwise. They may be downloaded and/or printed for private study, or other acts as permitted by national copyright laws. The publisher or other rights holders may allow further reproduction and re-use of the full text version. This is indicated by the licence information on the White Rose Research Online record for the item.

Takedown

If you consider content in White Rose Research Online to be in breach of UK law, please notify us by emailing eprints@whiterose.ac.uk including the URL of the record and the reason for the withdrawal request.

1
2
3
4
5
6
7
8
9
10
11
12
13
14
15
16
17
18
19
20
21
22
23
24
25
26
27
28
29
30
31
32
33
34
35
36
37
38
39
40
41
42
43
44
45
46
47

Differential Processing of the Direction and Focus of Expansion of Optic Flow Stimuli in areas MST and V3A of the Human Visual Cortex.

Running Title: Cortical Analysis of Optic Flow Stimuli

Samantha L. Strong^{a,b}, Edward H. Silson^{b,c}, André D. Gouws^b, Antony B. Morland^{b,d}
& Declan J. McKeefry^a

^aSchool of Optometry and Vision Science, University of Bradford, Bradford, West Yorkshire, BD7 1DP, UK.

^bYork Neuroimaging Centre, Department of Psychology, University of York, York, YO10 5DD, UK.

^cLaboratory of Brain and Cognition, National Institute of Mental Health, Bethesda, USA.

^dCentre for Neuroscience, Hull-York Medical School, University of York, York, YO10 5DD, UK.

Corresponding Author: Declan McKeefry

Email: d.mckeefry@bradford.ac.uk

Address: School of Optometry and Vision Science, University of Bradford, Bradford, West Yorkshire, BD7 1DP, UK

Tel: +44(0)1274 234648.

48 **Abstract**

49 Human neuropsychological and neuroimaging studies have raised the possibility that
50 different attributes of optic flow stimuli, namely radial direction and the position of the focus
51 of expansion (FOE), are processed within separate cortical areas. In the human brain, visual
52 areas V5/MT+ and V3A have been proposed as integral to the analysis of these different
53 attributes of optic flow stimuli. In order to establish direct causal relationships between neural
54 activity in V5/MT+ and V3A and the perception of radial motion direction and FOE position,
55 we used Transcranial Magnetic Stimulation (TMS) to disrupt cortical activity in these areas
56 whilst participants performed behavioural tasks dependent on these different aspects of optic
57 flow stimuli. The cortical regions of interest were identified in seven human participants using
58 standard fMRI retinotopic mapping techniques and functional localisers. TMS to area V3A
59 was found to disrupt FOE positional judgements, but not radial direction discrimination, whilst
60 the application of TMS to an anterior sub-division of hV5/MT+, MST/TO-2, produced the
61 reverse effects, disrupting radial direction discrimination but eliciting no effect on the FOE
62 positional judgement task. This double dissociation demonstrates that FOE position and
63 radial direction of optic flow stimuli are signalled independently by neural activity in areas
64 hV5/MT+ and V3A.

65 **Key Words:** transcranial magnetic stimulation, fMRI, psychophysics, V5/MT+, V3A.

66

67

68 **New and Noteworthy**

69 Optic flow constitutes a biologically relevant visual cue as we move through any
70 environment. Using neuro-imaging and brain-stimulation techniques this study demonstrates
71 that separate human brain areas are involved in the analysis of the direction of radial motion
72 and the focus of expansion in optic flow. This dissociation reveals the existence of separate
73 processing pathways for the analysis of different attributes of optic flow which are important
74 for the guidance of self-locomotion and object avoidance.

75 **Introduction**

76 When we move through our environment visual cues about the nature and direction of this
77 motion are provided by the changing pattern of images formed on our retinae – so called
78 optic flow. The ability of the human visual system to analyse optic flow is of crucial biological
79 significance as it provides key visual cues that can be used for the guidance of self-motion
80 and object avoidance (Gibson, 1950). Movement by an individual (typically forwards)
81 generates a focus of expansion (FOE) in optic flow from which all motion vectors expand and
82 this provides crucial information about heading direction (Warren & Hannon, 1988). Analysis
83 of the global nature and direction of radial motion, on the other hand, constitutes a very
84 different type of cue to that offered by the analysis of FOE position. The signalling of radial
85 motion provides information that can be used to globally subtract or parse flow motion, which
86 is essential for the tracking and avoidance of independently moving objects during self-
87 motion (Warren & Rushton, 2009).

88

89 Visually presented moving stimuli elicit neural activity across an extensive network of human
90 brain areas including: V1, V2, V3, V3A, V3B, hV5/MT+, V6, IPS0-4 (Zeki et al., 1991;
91 Watson et al., 1993; Tootell et al., 1997; Smith et al., 1998; Culham et al., 2001; Claeys et
92 al., 2003; Sieffert et al., 2003; Pitzalis et al., 2010). In the human brain, two cortical areas
93 within this network exhibit a particularly high sensitivity to visual motion. The first of these is
94 human V5/MT+ (hV5/MT+), and is the visual area most closely associated with motion
95 processing (Zeki et al., 1991; Watson et al., 1993; Tootell et al., 1995; Dumoulin et al., 2000;
96 Culham et al., 2001). hV5/MT+ forms a complex comprising at least two, but possibly more
97 visual areas (see: Kolster et al., 2010). These subdivisions have been tentatively proposed
98 as human homologues of areas MT and MST, which form constituents of V5/MT+ in the
99 monkey brain (Dukelow et al., 2001; Huk et al., 2002; Amano et al., 2009). In this study we
100 have adopted the terms MT/TO-1 for the posteriorly located area and MST/TO-2 for the
101 anterior sub-division. This nomenclature reflects the suggested functional homology with the

102 macaque as well their differentiation in the human brain on the basis of their retinotopic
103 characteristics (Amano et al., 2009). The other human visual area with a high degree of
104 motion selectivity is area V3A which contains a representation of the full contra-lateral visual
105 hemi-field and lies anterior and dorsal to area V3 in the occipito-parietal cortex. V3A is
106 second only to hV5/MT+ in terms of its sensitivity to motion stimuli (Tootell et al. 1997; Smith
107 et al., 1998; Vanduffel et al., 2002; Sieffert et al., 2003). This is in contrast to the monkey
108 brain where it is neurons in V3, rather than V3A, which are more responsive to motion stimuli
109 (Felleman & Van Essen, 1987).

110

111 Human neuropsychological studies have raised the possibility that the analysis of FOE
112 position and radial motion direction of optic flow stimuli occurs within separate cortical areas.
113 Beardsley & Vaina (2005), for example, demonstrated that a patient with damage to
114 hV5/MT+ was impaired in terms of their ability to perceive radial motion direction but their
115 ability to detect FOE position remained intact. Neuroimaging data also point to a segregation
116 of function with regards to the analysis of the radial direction of optic flow and FOE position.
117 Consistent with the functional specialisations that have been reported for monkey MT and
118 MST (Saito et al., 1986; Mikami et al., 1986; Komatsu and Wurtz, 1988; Duffy and Wurtz,
119 1991a; b; Tanaka et al., 1993, Lagae et al., 1994; Eifuku and Wurtz, 1998; Duffy, 1998) the
120 anterior subdivision of hV5/MT+, MST/TO2, has been shown to be selectively responsive to
121 radial motion or optic flow stimuli. MST/TO-2 appears to be more specialised for encoding
122 the global flow properties of complex motion stimuli in comparison to its posterior counterpart
123 MT/TO-1 (Smith et al., 2006; Wall et al., 2008). In terms of the analysis of FOE position,
124 neural activity in area V3A has been identified as potentially important. Koyama et al. (2005)
125 in their fMRI experiments demonstrated that activity within human V3A is closely correlated
126 with the position of FOE. Cardin et al. (2012) have also demonstrated sensitivity in V3A to
127 FOE position.

128 Both neuropsychological and neuroimaging data have their limitations. In the case of the
129 former, lesions are rarely confined to discrete visual areas, whilst the latter provide only
130 correlative measures of brain function. As a result it is neither possible to ascertain from
131 these results whether the perception of FOE position is causally dependent on neural activity
132 in area V3A, nor whether a similar causal relationship exists between neural activity in
133 hV5/MT+ and the perception of radial direction in optic flow. Therefore the purpose of this
134 study was to test the hypothesis that human cortical areas hV5/MT+ (more specifically its
135 anterior sub-division, MST/TO-2) and V3A perform distinct and separable contributions to the
136 perception of radial motion direction and FOE position of optic flow stimuli. In order to
137 establish causal dependencies, we used repetitive Transcranial Magnetic Stimulation (rTMS)
138 to disrupt neural function within hV5/MT+ and V3A whilst participants performed behavioural
139 tasks that assessed the ability of human observers to discriminate the direction of radially
140 moving dots or changes in the position of FOE in optic flow stimuli. All cortical target sites
141 were identified in each of the participants using fMRI retinotopic mapping procedures
142 (Serenio et al., 1995; DeYeo et al., 1996; Engel et al., 1997) combined with functional
143 localisers (Dukelow et al., 2001; Huk et al., 2002; Amano et al., 2009).

144

145 **Materials and Methods**

146 **Participants**

147 Seven volunteers participated in this study (five male; ages 21-48). All participants had
148 normal or corrected-to-normal vision at the time of testing and gave written informed
149 consent. Experiments were approved by ethics committees at both the University of Bradford
150 and York Neuroimaging Centre, and were carried out in accordance with the Declaration of
151 Helsinki and accepted TMS safety protocols (Wassermann, 1998; Lorberbaum and
152 Wassermann, 2000; Rossi et al., 2009).

153

154

Figure 1 here

155

156 **Visual Stimuli**

157 Visual stimuli were presented on a 19-inch Mitsubishi DiamondPro 2070SB monitor (refresh
158 rate 75Hz; 1024 x 768 resolution) and consisted of moving white dots (size: $\sim 0.2^\circ$; density:
159 $4.69/\text{deg}^2$) within a 10° (diameter) circular aperture. The constituent dots moved at a speed
160 of $7^\circ/\text{s}$ (with a flat speed gradient) and were presented for 200ms on each trial. In experiment
161 1, the radial motion stimuli comprised signal and noise dots. A percentage of the dots were
162 signal dots that moved coherently in a radial direction (expanding/contracting). The exact
163 percentage of signal dots was set (for each individual) at a level corresponding to the 75%
164 correct performance threshold for the radial direction discrimination task. This was
165 determined in preliminary psychophysical experiments. Across all the observers 75% correct
166 performance typically required relatively low percentages of signal dots (range: 10.1 -
167 24.4%). The remaining (noise) dots moved in random directions and had a uniform density
168 across the stimulus aperture. In experiment 2 a similar radial motion aperture stimulus was
169 placed within a hemi-field of randomly moving dots and FOE position of this stimulus could
170 be moved upwards or downwards (see Figure 1). The magnitude of the FOE displacement
171 corresponded to 75% correct performance, which was also determined in preliminary
172 psychophysical experiments. In order to prevent any confounding effects that could arise if
173 the signal dots created a perceptual border at the intersection with the noise dots, a
174 coherence level of 70% for the signal dots in the radial motion aperture stimulus was used.
175 When the stimulus was placed within the hemi-field of randomly moving noise dots, this
176 effectively masked the presence of any motion-defined border between the aperture stimulus
177 and the background. To control for any potential cues arising from the difference in density of
178 the expanding dots at the FOE versus the periphery; 10% of the 70% coherent signal dots
179 were contracting towards a common focal point whilst the remainder were expanding in the
180 opposite direction.

181

182 The centres of motion stimuli were positioned 15° to the left of fixation for both
183 TMS/behavioural experiments. This placement was used in order to minimise involvement of
184 ipsi-lateral V5/MT+ in the performance of the motion discrimination tasks as Amano et al
185 (2009), for example, have demonstrated that the receptive fields of hV5/MT+ neurones can
186 extend well beyond the vertical meridian into the ipsi-lateral (in this case the left) visual field.

187

188

189 **fMRI Localisation of Cortical ROIs**

190 All functional and structural magnetic resonance imaging scans were acquired using a GE 3-
191 Tesla Sigma Excite HDX scanner. The multi-average, whole-head T1-weighted structural
192 scans for each participant encompassed 176 sagittal slices (repetition time (TR) = 7.8ms,
193 echo time (TE) = 3ms, inversion time (TI) = 450ms, field of view (FOV) = 290 x 290 x 276,
194 256 x 256 x 176 matrix, flip angle = 20° , $1.13 \times 1.13 \times 1.0\text{mm}^3$). The functional MRI scan
195 used a gradient recalled echo pulse sequences to measure T2 weighted images (TR =
196 3000ms, TE = 29ms, FOV = 192cm, 128x128 matrix, 39 contiguous slices, $1.5 \times 1.5 \times$
197 1.5mm^3 , interleaved slice order with no gap).

198

199 Two sub-divisions of hV5/MT+ (MT/TO-1 and MST/TO-2) were identified using techniques
200 similar to those described previously (Dukelow et al., 2001; Huk et al., 2002; Amano et al.,
201 2009). Briefly, localiser stimuli consisting of a 15° aperture of 300 moving white dots ($8^\circ/\text{s}$)
202 were centrally displaced 17.5° relative to a central fixation target into either the left or right
203 visual field. By contrasting responses to moving with those to static, MST/TO-2 was
204 identified by ipsi-lateral activations to stimulation of either the right or left visual field. MT/TO-
205 1 was located by subtracting the anterior MST/TO-2 activity from the whole hV5/MT+
206 complex activation found for contra-lateral stimulation (Dukelow et al., 2001; Huk et al.,
207 2002; Amano et al., 2009; Strong et al., 2016). Stimuli in this case were projected onto a
208 rear-projection screen and viewed through a mirror (refresh rate 120Hz; 1920 x 1080
209 resolution; viewing distance 57cm).

210

211 Standard retinotopic mapping techniques (Serenio et al., 1995; DeYeo et al., 1996; Engel et
212 al., 1997) using a 90° anti-clockwise rotating wedge (flicker rate 6Hz), and an expanding
213 annulus ($\leq 15^\circ$ radius), both lasting 36s per cycle, were used to identify area V3A and the
214 control site LO-1, in each participant. Area V3A, located in superior occipito-parietal cortex,
215 contains a complete hemi-field representation of the contra-lateral visual field. This
216 differentiates it from dorsal and ventral V2 and V3, which map only a quadrant of the contra-
217 lateral field (Tootell et al., 1997). LO-1 lies ventral to V3A and contains a lower contra-lateral
218 visual field map posteriorly, and an upper contra-lateral visual field representation anteriorly
219 (see Figure 2). LO-1 was chosen as a control site because it lies in close proximity to areas
220 V3A and hV5/MT+, but unlike them, is largely unresponsive to visual motion (Larsson &
221 Heeger, 2006) and exhibits only weak activation in response to moving stimuli (Bartels et al.,
222 2008). Brainvoyager QX (Brain Innovation, Maastricht) was used to analyse the fMRI data
223 and to identify target sites for the TMS, which were selected as centre-of-mass co-ordinates
224 for identified ROIs. Table 1 provides Talairach co-ordinates for each of the target sites (right
225 hemisphere only) in all 7 participants.

226

227 *Figure 2 here* *Table 1 here*

228

229 **TMS Stimulation**

230 The TMS coil was positioned over the cortical test and control sites identified from the fMRI
231 localisation and retinotopic mapping experiments described above. In these experiments
232 TMS was delivered to the target sites in the right hemisphere. Following identification of
233 these target points in 3D space, co-registration between the subject's head and the structural
234 scans was achieved using a 3D ultrasound digitizer (CMS30P (Zebris)) in conjunction with
235 the BrainVoyager software. This allowed coil position to be monitored and adjusted
236 throughout the experiment by creating a local spatial co-ordinate system which links the

237 spatial positions of ultrasound transmitters on the subject and the coil with pre-specified
238 fiducials on the structural MRIs (see: McKeefry et al., 2008).

239

240 During the behavioural experiments TMS pulses were delivered using a Magstim RapidPro 2
241 (Magstim, UK) figure-of-eight coil (50mm). During each trial a train of five biphasic pulses
242 was applied (see Figure 1). This pulse train had a total duration of 200ms and the pulse
243 strengths were set at 70% maximal stimulator output. The onsets of the pulse trains were
244 synchronous with the onset of the presentation of test stimuli.

245

246

247 **Psychophysical/TMS Experimental Procedures**

248 Participants viewed the monitor with their right eye at a distance of 57cm with the left eye
249 occluded and head restrained in a chin rest. All trials for Experiment 1 and Experiment 2
250 were set to the 75% threshold abilities of each participant. In these preliminary experiments,
251 a method of constant stimuli (MOCS) was used to determine threshold, with 50 repetitions of
252 each coherence level between 5-50% for the radial motion task, and 30 repetitions of each
253 position change between -1 - +1 degree of visual angle for the FOE task.

254

255 In the combined behavioural/TMS experiments we employed a 2-AFC procedure and the
256 order of conditions (each comprising 100 trials) was counter-balanced across participants
257 and TMS was applied single-blind. In experiment 1, participants indicated whether the dots
258 were moving inwards (contracting) or outwards (expanding). In experiment 2, participants
259 viewed a reference stimulus comprising a similar aperture of radially expanding dots placed
260 within a field of random dots (see figure paradigm). The FOE was level with fixation but was
261 displaced in the left visual field. In a second presentation (test stimulus) the FOE was
262 displaced either up or down at a distance set to threshold (75%) performance. Participants
263 indicated the direction positional change perceived by an appropriate keyboard button press

264 and were instructed to respond as quickly and accurately as possible. Response time was
265 measured as the time taken for the participant to press one of the decision keys on the
266 keyboard following stimulus offset.

267

268 Statistical analysis of the results for each task was carried out using IBM SPSS Statistics 20,
269 using repeated measure ANOVAs. The assumption of normal distribution was confirmed with
270 Mauchly's Test of Sphericity. If this assumption was violated, the degrees of freedom (dF)
271 were corrected to allow appropriate interpretation of the F value of the ANOVA. These
272 corrections included the Greenhouse-Geisser when sphericity (ϵ) was reported as less than
273 0.75, and Huynh-Feldt correction when sphericity exceeded 0.75.

274

275

276 **Results**

277 Group averaged performance was expressed in terms of percent correct (pCorrect) for each
278 of the TMS conditions as well as for a baseline condition (when no TMS was administered
279 whilst the participants performed the task). Inspection of Figure 3 reveals that relative to all
280 other TMS conditions, stimulation of MST/TO-2 results in a loss of performance in radial
281 direction discrimination, whereas discrimination of FOE is impaired only for TMS applied to
282 V3A. These effects are examined statistically below.

283

284 As these tasks were designed to measure two different aspects of optic flow processing, the
285 data were interrogated for any interactions using a two-way ANOVA comparing TMS site
286 with tasks in order to investigate independence from one another. This analysis highlighted a
287 significant interaction between TMS site and the tasks we examined in experiments 1 and 2
288 ($F(3,48) = 5.98, p = 0.002$). Significant differences were also found across tasks ($F(1,48) =$
289 $4.57, p = 0.038$) and TMS sites ($F(3,48) = 5.08, p = 0.004$). This shows that results were
290 significantly different between tasks and TMS conditions.

291

292

Figure 3 here

293

294 In order to examine the main effect of TMS site on performance for each task separately,
295 repeated-measures ANOVAs were also used. For the radial motion direction discrimination,
296 a significant effect of TMS condition on task performance was found ($F(3,18) = 13.55$, $p <$
297 0.001). Pair-wise comparisons (Bonferroni-corrected) for this task indicated that this effect
298 was due to significant differences existing between Baseline and MST/TO-2 ($p = 0.018$),
299 Control and MST/TO-2 ($p = 0.012$), and, crucially, V3A and MST/TO-2 ($p = 0.015$). All other
300 comparisons failed to demonstrate any significant differences (Baseline *versus* Control, $p =$
301 0.448 ; all other comparisons, $p = 1.00$) (see figure 3a). These results demonstrate that
302 neural processing in area MST/TO-2 appears to be essential for normal levels of
303 performance for the radial motion direction discrimination task. Conversely, disruption to
304 neural activity in area V3A has no effect on performance levels for this task.

305

306 Similar analyses applied to the data obtained in the FOE displacement experiment
307 demonstrated show the opposite effects for areas MST/TO-2 and V3A. There is a significant
308 main effect of TMS site on performance on the FOE task ($F(3,18) = 15.36$, $p < 0.001$).
309 Subsequent pair-wise comparisons (Bonferroni-corrected) highlighted significant differences
310 between Baseline and V3A ($p = 0.005$), Control and V3A ($p = 0.019$), and MST/TO-2 and
311 V3A ($p = 0.031$), highlighting the key role of V3A in FOE processing. No other comparisons
312 were found to be significantly different (all other comparisons equated to $p = 1.00$) (see
313 figure 3b).

314

315 Average response times are plotted in Figure 4 and were analysed to investigate for

316 potential differences between TMS conditions. Repeated-measures ANOVAs demonstrated
317 no significant effects of TMS site on speed of response for experiment 1 ($F(3,18) = 0.80, p =$
318 0.509) or experiment 2 ($F(3,18) = 2.15, p = 0.129$). If subjects responded quickly at the cost
319 of accuracy, this could have confounded our accuracy results. To investigate this, percent
320 correct was correlated against response times (see Table 2). Evidence of a positive
321 correlation would imply that a speed-accuracy trade-off may have been present, whereas
322 evidence of a negative correlation would suggest that slow responses were potentially due to
323 more difficult trials.

324

325 *Figure 4 here Table 2 here*

326

327 The data are plotted in figure 5 and Pearson's R analyses identified a moderate negative
328 correlation between percent correct and response time for experiment 1 ($r = -0.36, n = 28, p$
329 $= 0.061$) but no significant relationship for experiment 2 ($r = -0.20, n = 28, p = 0.305$). It is
330 important to note that while one of the correlations is not significant and the other
331 approaches significance, they are both negative indicating that if a relationship between the
332 speed of response and accuracy exists, it is one that is in the opposite direction to a 'speed-
333 accuracy' trade off. We are confident therefore that the results of our analysis of the
334 accuracy data (above) are not confounded by reaction times as there is no evidence for
335 faster response times resulting in poorer performance.

336

337 *Figure 5 here*

338

339

340

341 **Discussion**

342 In this study we have demonstrated that the perception of different attributes of optic flow
343 stimuli, namely, radial direction and FOE position, are dependent upon neural activity within
344 separate visual areas within the human cerebral cortex. We have established that there is a
345 direct causal relationship between neural activity in area MST/TO-2, a sub-division of
346 hV5/MT+ complex, and the perception of the direction of radial motion. In addition, a similar
347 dependency exists between neural activity in area V3A and the perception of FOE position.
348 Importantly, we have shown a double dissociation between the involvement of visual areas
349 V3A and MST/TO-2 in the analysis of these different aspects of optic flow stimuli which
350 indicates that the processing of FOE position and radial motion direction occur independently
351 of one another within these separate cortical areas.

352

353 Expanding (radial) motion is naturally apparent when an individual moves forwards through
354 space. This optic flow constitutes a rich source of visual cues that can facilitate navigation
355 through external environments. In static environments analysis of the FOE can provide
356 information about the direction in which the individual is travelling (Warren & Hannon, 1988).
357 However, in more dynamic surroundings the importance of global directional properties of
358 optic flow in the process of 'flow parsing' has also been highlighted (Warren & Rushton
359 2009). This process allows signals that are generated by self-movement to be discounted in
360 order to identify the motion of objects within a scene that are moving independently. This
361 complimentary visual information is essential for the tracking and avoidance of objects during
362 self-motion. Appropriate interpretation of all these cues is essential for successful navigation
363 of the external world. Of course in addition to visual, there are a number of other non-visual
364 cues that also contribute to the perception of self-motion (Royden et al., 1992; Bradley et al.
365 1996; Gu et al., 2006; Fetsch et al., 2007; Cardin & Smith, 2010; Kaminiarz et al., 2014). But
366 if we restrict our consideration to visual cues only, the importance of optic flow appears to be
367 highlighted by the fact that many cortical areas are responsive to such stimuli. Human

368 neuroimaging studies have shown that hV5/MT+, V3A, V3B, V6, ventral intraparietal area
369 (VIP) and the cingulate sulcus visual area (CSv) are all activated by optic flow (Smith et al.,
370 2006; Cardin et al., 2012; Morrone et al., 2000; Wall & Smith, 2009; Pitzalis et al 2013a). The
371 stimuli used in these and other behavioural (e.g. Warren & Hannon, 1988) and
372 neurophysiological (e.g. Zang & Britten, 2010) studies into the mechanisms of self-motion
373 guidance and perception have typically employed centrally viewed, large-field optic flow
374 stimuli. In comparison, the stimuli used in this study are spatially constrained and, as a
375 result, are unlikely to provide cues for the guidance of self-motion that are as powerful as
376 those derived from more extensive optic flow fields. The small aperture stimuli lack the
377 richness of all the visual as well as non-visual cues that are provided by optic flow stimuli
378 observed under more naturalistic viewing conditions. For example, there is no sense of
379 “vection”, the perception of self-movement through space, generated by these small field
380 stimuli. But despite their relative sparseness, the aperture stimuli used in these experiments
381 are sufficient to reveal the existence of important functional differences between the earliest
382 stages of this processing network, with areas MST/TO-2 and V3A playing different roles in
383 the analysis of radial flow direction and FOE position, respectively. This functional
384 segregation is important in that it may help to explain results from neuropsychological case
385 studies. Beardsley and Vaina, for example, examined a patient (GZ) who suffered damage to
386 her right hV5/MT+ complex. As a result of this lesion, GZ was impaired in her ability to
387 discriminate the radial direction of optic flow stimuli, but her ability to determine the position
388 of their FOE remained intact (Beardsley & Vaina, 2005). The results presented here raise the
389 possibility that this preservation of function is due to the fact that the neural processing that
390 underpins the perception of these different attributes of optic flow is localised within separate
391 cortical locations. The preservation of FOE perception may be attributable to the fact that
392 that if V3A remains intact in patient GZ, this would be sufficient to support the perception of
393 FOE position, even in the absence of hV5/MT+.

394

395 In the monkey brain, investigation of the physiological substrates of self-motion perception
396 has centred on area MST (Britten 2008). Neurons in the dorsal region of MST (MSTd) are
397 tuned to complex patterns of optic flow that result from self-motion (Saito et al., 1986;
398 Tanaka et al 1986; 1989; Duffy & Wurtz, 1991; 1995). Importantly, a causal dependency has
399 been firmly established between neural activity in this area and the perception of heading
400 direction in monkeys (Britten & Van Wezel, 1998; 2002; Gu et al., 2006; 2007; 2008; 2012;
401 Yu et al., 2017). The lack of any disruption to FOE positional judgments when the human
402 homolog of MST is disrupted by TMS therefore presents something of an inconsistency
403 between human and monkey data. A possible explanation for the lack of effect reported here
404 might lie in our fMRI localizer paradigms for MST/TO-2. It is conceivable that whilst neurons
405 in MST/TO-2 are activated by ipsi-lateral stimuli, some will have much stronger response
406 biases to contra-lateral stimuli. This potentially might lead to some voxels which are
407 genuinely part of MST/TO-2 being misclassified as falling within the MT/TO-1 sub-division of
408 hV5/MT+. This could feasibly lead to an under-estimation of the extent of MST/TO-2 and
409 failure to localize it properly. However, we consider this unlikely for a number of reasons.
410 Firstly, previous studies have demonstrated a high degree of correspondence between
411 functional data and population receptive field maps (Amano et al., 2009), which gives us
412 confidence that the localiser used here is an appropriate method for identifying MT/TO-1 and
413 MST/TO-2. Secondly, the Talairach co-ordinates from our centre-of-mass target points for
414 MT/TO-1 and MST/TO-2 are similar to those previously reported for these regions (Dukelow
415 et al., 2001; Kolster et al., 2010). Finally, the use of the current fMRI localisers has
416 previously enabled successful functional differentiation between MT/TO-1 and MST/TO-2
417 where selective effects have been demonstrated for radial motion direction discrimination
418 tasks following the application of TMS to these regions (Strong et al., 2016).

419

420 The lack of any effect of disruption to MST/TO-2 of FOE positional judgements would appear
421 to suggest that human MST/TO-2 may not be critical for the perception of the direction of

422 self-motion. This is in agreement with studies that have shown human MST/TO-2 to be
423 responsive to optic flow stimuli regardless of whether they were compatible with the
424 perception of self-motion or not (Wall & Smith, 2008). However, an alternative explanation
425 for the apparent lack of involvement of human MST/TO-2 in FOE judgements might lie in the
426 fact that the task in experiment 2 requires the detection of a change in FOE position. In the
427 macaque, MSTd neurons are insensitive to temporal changes in heading direction signaled
428 by FOE positional shifts (Paolini et al 2000). Human MST/TO-2, whilst clearly being
429 responsive to optic flow stimuli (Smith et al., 2006; Wall et al., 2008; Strong et al., 2016),
430 shows a similar lack of sensitivity to changes in FOE position (Furlan et al. 2014). The
431 detection of such changes are important in that they signal shifts in heading direction as
432 opposed to providing information relating to instantaneous heading direction (Furlan et al.,
433 2014). Results from this study implicate V3A as an area that is critical for signaling these
434 transient changes in FOE position. This is consistent with previous findings. For example,
435 studies by Koyama et al. (2005) and Cardin et al. (2012) have both shown that fMRI signal
436 increases in V3A are elicited by changes in position of the FOE. Furthermore, this function
437 may form part of a wider role in the analysis and prediction of the position of moving objects
438 that has been proposed for area V3A (Maus et al., 2010).

439

440 V3A has been given relatively little consideration in the context of self-motion perception in
441 the monkey brain (see: Britten, 2008). This may be due to differences in the role of area V3A
442 across the species (Gaska et al., 1988; Girard et al., 1991; Galletti et al., 1990; Tootell et al.,
443 1997; Orban et al., 2003; Tsao et al., 2003; Anzai et al., 2011). In humans, area V3A has
444 been shown to be highly responsive to moving stimuli forming a much more prominent
445 constituent of the cortical network that exists for motion processing (Tootell et al., 1997;
446 McKeefry et al., 2008; 2010). Nonetheless, V3A is still considered sub-ordinate to area
447 hV5/MT+ in this motion processing hierarchy (see: Felleman & Van Essen 1991; Britten
448 2008). However, the results presented here challenge this strict hierarchy by showing that

449 neural activity in V3A can support the perception of specific attributes of moving stimuli, even
450 in the absence of a normally functioning hV5/MT+. The analysis of optic flow does not simply
451 occur in a serial fashion with information passing from V3A to hV5/MT+ for further
452 processing. Instead, our results, consistent with neuropsychological reports, point to the
453 existence of parallel processing pathways for radial direction and FOE positional change.
454 MST/TO-2 and V3A would appear to form important initial stages in the processing of these
455 two key attributes of optic flow stimuli that can ultimately be used in flow parsing and signal
456 heading direction, both of which make important contributions to the guidance of self-
457 movement.

458

459 The notion of multiple motion processing pathways emanating from early visual areas is
460 compatible with previous studies (Pitzalis et al., 2010; 2013b,c, 2015) but carries with it the
461 implication that signals from these pathways must be combined at some later stage. In both
462 humans and monkeys other 'higher' brain areas have been identified as possible subsequent
463 stages in the perception of self-motion. One such area is V6, which is found in the medial
464 parieto-occipital sulcus and is thought to be involved in the analysis of self-motion relative to
465 object motion in dynamic environments (Galletti et al., 1990; 2001; Shipp et al., 1998; Pitzalis
466 et al., 2010; 2013a,b,c, 2015; Cardin & Smith, 2011; Fischer et al., 2012; Cardin et al., 2012;
467 Fan et al., 2015). V6 does not appear to exhibit sensitivity to changes in FOE position
468 (Cardin et al., 2012; Furlan et al., 2014) and as a result is considered more important in flow
469 parsing for the purposes of object avoidance during self-motion, rather than heading
470 direction analysis per se (Cardin et al., 2012). Another key region is the polysensory ventral
471 intraparietal area (VIP). In monkeys, VIP contains neurons that have very similar response
472 properties to those found in MSTd and are important in the encoding of heading direction
473 (Schaafsma & Duysens, 1996; Bremmer et al., 2002; Zhang & Britten, 2010, 2011). The
474 putative human homologue of VIP has also been shown to be responsive to egomotion
475 compatible optic flow and changes in FOE position (Wall & Smith 2008; Furlan et al, 2014).

476 In the human brain, VIP along with another cortical region found on the cingulate gyrus, CSv,
477 have been identified as key areas in a pathway involved in the analysis of instantaneous
478 changes in FOE position as a means of computing heading direction (Furlan et al., 2014).
479 The extent to which neural activity in these higher human cortical areas can be causally
480 related to flow parsing mechanisms or to the perception of heading direction remains to be
481 determined. But results from this study would suggest that at a relatively early stage there is
482 evidence of segregated processing for FOE position and radial motion direction in optic flow
483 stimuli. This segregation may persist in areas V6, VIP and CSv as a means to support the
484 different requirements for the analysis and guidance of self-motion.

485

486 **Acknowledgements**

487 This work was funded by the BBSRC (grant B/N003012/1). We thank William McIlhagga for
488 comments on previous versions of this paper.

489

490 **References**

- 491 **Amano K, Wandell BA, Dumoulin SO.** Visual field maps, population receptive field sizes,
492 and visual field coverage in the human MT+ complex. *J Neurophysiol* 102: 2704-2718, 2009.
- 493 **Anzai A, Chowdhury SA, DeAngelis GC.** Coding stereoscopic depth information in visual
494 areas V3 and V3A. *J Neurosci* 31: 10270-10282, 2011.
- 495 **Bartels A, Zeki S, Logothetis NK.** Natural vision reveals regional specialization to local
496 motion and to contrast-invariant, global flow in the human brain. *Cereb Cortex* 18: 705-717,
497 2008.
- 498 **Beardsley SA, Vaina LM.** How can a patient blind to radial motion discriminate shifts in the
499 center-of-motion? *J Comp Neurosci* 18: 55-66, 2005.
- 500 **Bradley DC, Maxwell M, Andersen RA, Banks MS, Shenoy KV.** Mechanisms of heading
501 perception in primate visual cortex. *Science* 273: 1544–1547, 1996.
- 502 **Bremmer F, Duhamel JR, Ben Hamed S, Graf W.** Heading encoding in the macaque
503 ventral intraparietal area (VIP). *Eur J Neurosci* 16: 1554–68, 2002.
- 504 **Britten KH.** Mechanisms of self-motion perception. *Ann Rev Neurosci* 31: 389–410, 2008.
- 505 **Britten KH, van Wezel RJ.** Electrical microstimulation of cortical area MST biases heading
506 perception in monkeys. *Nat Neurosci* 1: 59-63, 1998.
- 507 **Britten KH, van Wezel RJ.** Area MST and heading perception in macaque monkeys. *Cereb*
508 *Cortex* 12: 692–701, 2002.
- 509 **Cardin V, Smith AT.** Sensitivity of human visual and vestibular cortical regions to
510 egomotion-compatible visual stimulation. *Cereb Cortex* 20: 1964–1973, 2010.
- 511 **Cardin V, Smith AT.** Sensitivity of human visual cortical area V6 to stereoscopic depth
512 gradients associated with self-motion. *J Neurophysiol* 106: 1240-1249, 2011.
- 513 **Cardin V, Hemsworth L, Smith AT.** Adaptation to heading direction dissociates the roles of
514 human MST and V6 in the processing of optic flow. *J Neurophysiol* 108: 794-801, 2012.
- 515 **Claeys KG, Lindsey DT, De Schutter E, Orban GA.** A higher order motion region in human
516 inferior parietal lobule: evidence from fMRI. *Neuron* 40: 631-642, 2003.
- 517 **Culham J, He S, Dukelow S, Verstraten FAJ.** Visual motion and the human brain: what
518 has neuroimaging told us? *Acta Psychol* 107: 69-94, 2001.
- 519 **DeYoe EA, Carman GJ, Bandettini P, Glickman S, Wieser J, Cox R, Miller D, Neitz J.**
520 Mapping striate and extra-striate visual areas in human cerebral cortex. *Proc Natl Acad Sci*
521 *(USA)* 93: 2382–2386, 1996.
- 522 **Dukelow SP, DeSouza JFX, Culham JC, van den Berg AV, Menon RS, Vilis T.**
523 Distinguishing subregions of the human MT+ complex using visual fields and pursuit eye
524 movements. *J Neurophysiol* 86: 1991-2000, 2001.

- 525 **Duffy CJ.** MST neurons respond to optic flow and translational movement. *J Neurophysiol*
526 80: 1816-1827, 1998.
- 527 **Duffy CJ, Wurtz RH.** Sensitivity of MST neurons to optic flow stimuli. I. A continuum of
528 response selectivity to large-field stimuli. *J Neurophysiol* 65: 1329 –1345, 1991.
- 529 **Duffy CJ, Wurtz RH.** Response of monkey MST neurons to optic flow stimuli with shifted
530 centers-of-motion. *J Neurosci* 15: 5192-5208, 1995.
- 531 **Dursteler MR, Wurtz RH.** Pursuit and optokinetic deficits following chemical lesions of
532 cortical areas MT and MST. *J Neurophysiol* 60: 940-965, 1988.
- 533 **Eifuku S, Wurtz RH.** Response to motion in extra-striate area MST1: Center-surround
534 interactions. *J Neurophysiol* 80: 282-296, 1998.
- 535 **Engel SA, Glover GH, Wandell BA.** Retinotopic organization in human visual cortex and
536 the spatial precision of functional MRI. *Cereb Cortex* 7: 181-192, 1997.
- 537 **Fan RH, Liu S, DeAngelis GC, Angelaki DE.** Heading tuning in Macaque Area V6. *J*
538 *Neurosci* 35: 16303-16314, 2015.
- 539 **Fischer E, Bulthoff HH, Logothetis NK, Bartels A.** Human areas V3A and V6 compensate
540 for self-induced planar visual motion. *Neuron* 73: 1228-1240, 2012.
- 541 **Felleman DJ, Van Essen DC.** Receptive field properties of neurons in area V3 of macaque
542 monkey extrastriate cortex. *J Neurophysiol* 57: 889-920, 1987.
- 543 **Felleman DJ, Van Essen DC.** Distributed hierarchical processing in the primate cerebral
544 cortex. *Cereb Cortex* 1: 1–47, 1991.
- 545 **Fetsch CR, Wang S, Gu Y, DeAngelis GC, Angelaki D.** Spatial reference frames of visual,
546 vestibular and multi-modal heading signals in the dorsal subdivision of the medial superior
547 temporal area. *J Neurosci* 27: 700-712, 2007.
- 548 **Furlan M, Wann JP, Smith AT.** A representation of changing heading direction in human
549 cortical areas pVIP and CSv. *Cereb Cortex* 24: 2848-2858, 2014.
- 550 **Gaska JP, Jacobson LD, Pollen DA.** Spatial and temporal frequency selectivity of neurons
551 in visual cortical area V3A of the macaque monkey. *Vis Res* 28: 1179-1191, 1988.
- 552 **Gibson JJ.** The perception of the visual world. Boston (MA): Houghton Mifflin, 1950.
- 553 **Girard P, Salin PA, Bullier J.** Visual activity in areas V3a and V3 during reversible
554 inactivation of area V1 in the macaque monkey. *J Neurophysiol* 66:1493-1503, 1991.
- 555 **Galletti C, Battaglini PP, Fattori P.** 'Real-motion' cells in area V3A of macaque visual
556 cortex. *Exp Brain Res* 82: 67-76, 1990.
- 557 **Galletti C, Gamberini M, Kutz DF, Fattori P, Luppino G, Matelli M.** The cortical
558 connections of area V6: An occipitoparietal network processing visual information. *Eur J*
559 *Neurosci* 13: 1572-1588, 2001.

560 **Gu Y, Watkins PV, Angelaki DE, DeAngelis GC.** Visual and nonvisual contributions to
561 three-dimensional heading selectivity in the medial superior temporal area. *J Neurosci* 26:
562 73–85, 2006.

563 **Gu Y, DeAngelis GC, Angelaki DE.** A functional link between area MSTd and heading
564 perception based on vestibular signals. *Nat Neurosci* 10: 1038-1047, 2007.

565 **Gu Y, Angelaki DE, DeAngelis GC.** Neural correlates of multisensory cue integration in
566 macaque MSTd. *Nat Neurosci* 11: 1201–1210, 2008.

567 **Gu Y, DeAngelis GC, Angelaki DE.** Causal links between dorsal medial superior temporal
568 area neurons and multisensory heading perception. *J Neurosci* 32: 2299-2313, 2012.

569 **Huk AC, Dougherty RF, Heeger DJ.** Retinotopy and functional subdivision of human areas
570 MT and MST. *J Neurosci* 22: 7195-7205, 2002.

571 **Kaminiaz A, Schlack A, Hoffman K-P, Lappe, M, Bremmer F.** Visual selectivity for
572 heading in the macaque ventral intraparietal area. *J Neurophysiol* 112: 2470-2480, 2014.

573 **Komatsu H, Wurtz RH.** Relation of cortical areas MT and MST to pursuit eye movements. I.
574 Localization and visual properties of neurons. *J Neurophysiol* 60: 580-603, 1988.

575 **Komatsu H, Wurtz RH.** Modulation of pursuit eye movements by stimulation of cortical
576 areas MT and MST. *J Neurophysiol* 62: 31-47, 1989.

577 **Koyama S, Sasaki Y, Andersen GJ, Tootell RBH, Matsuura M, Watanabe T.** Separate
578 processing of different global-motion structures in visual cortex is revealed by fMRI. *Curr Biol*
579 15: 2027-2032, 2005.

580 **Lagae L, Maes H, Raiguel S, Xiao D-K, Orban GA.** Responses of macaque STS neurons
581 to optic flow components: a comparison of areas MT and MST. *J Neurophysiol* 71: 1597–
582 1626, 1994.

583 **Larsson J, Heeger DJ.** Two retinotopic visual areas in human lateral occipital cortex. *J*
584 *Neurosci* 26: 13128-13142, 2006.

585 **Lorberbaum JP, Wassermann E.** Safety concerns of TMS. Transcranial Magnetic
586 Stimulation in Neuropsychiatry. Edited by George, M.S., Belmaker, R.H. Washington D.C.,
587 American Psychiatric Press, 141-161, 2000.

588 **Maus GW, Weigelt S, Nijhawan R, and Muckli L.** Does area V3A predict positions of
589 moving objects? *Front Psychol* doi: 10.3389/fpsyg.2010.00186

590 **McKeefry DJ, Watson JDG, Frackowiak RSJ, Fong K, Zeki S.** The activity in Human
591 areas V1, V2, V3 and V5 during the perception of coherent and incoherent motion.
592 *Neuroimage*. 5: 1-12, 1997.

593 **McKeefry DJ, Burton MP, Vakrou C, Barrett BT, Morland AB.** Induced deficits in speed
594 perception by transcranial magnetic stimulation of human cortical areas V5/MT+ and V3A. *J*
595 *Neurosci* 28: 6848-6857, 2008.

596 **McKeefry DJ, Burton, MP, Morland A.** The contribution of human cortical area V3A to the
597 perception of chromatic motion: a transcranial magnetic stimulation study. *Eur J Neurosci* 31:
598 575-584, 2010.

599 **Mikami A, Newsome WT, Wurtz RH.** Motion selectivity in macaque visual cortex. I.
600 Mechanisms of direction and speed selectivity in extrastriate area MT. *J Neurophysiol*
601 55:1308-1327,1986.

602 **Morrone MC, Tosetti M, Montanaro D, Fiorentini A, Cioni G, Burr DC.** A cortical area that
603 responds specifically to optic flow, revealed by fMRI. *Nat Neurosci* 3: 1322–1328, 2000.

604 **Orban GA, Fize D, Peuskens H, Denys K, Nelissen K, Sunaert S, Todd J, Vanduffel W.**
605 Similarities and differences in motion processing between the human and macaque brain:
606 evidence from fMRI. *Neuropsychologia*. 41: 1757-1768, 2003.

607 **Paolini M, Distler C, Bremmer F, Lappe M, Hoffmann KP.** Responses to continuously
608 changing optic flow in area MST. *J Neurophysiol* 84: 730–43, 2000.

609 **Pitzalis S, Sdoia S, Bultrini A, Committeri G, Di Russo F, Fattori P, Galletti C, Galati G.**
610 Selectivity to translational egomotion in human brain motion areas. *PLoS ONE* 8: e60241.
611 doi:10.1371/journal.pone.0060241, 2013.

612 **Pitzalis S, Sereno MI, Committeri G, Fattori P, Galati G, Patria F, Galletti C.** Human V6:
613 the medial motion area. *Cereb Cortex* 20: 411-424, 2010.

614 **Pitzalis S, Fattori P, Galletti C.** The functional role of the medial motion area V6. *Front*
615 *Behav Neurosci* doi: 10.3389/fnbeh.2012.00091, 2013a.

616 **Pitzalis S, Bozzacchi C, Bultrini A, Fattori P, Galletti C, Di Russo F.** Parallel motion
617 signals to the medial and lateral motion areas V6 and MT+. *Neuroimage* 67: 89-100, 2013b.

618 **Rossi S, Hallett M, Rossini PM, Pascual-Leone A.** Safety, ethical considerations, and
619 application guidelines for the use of transcranial magnetic stimulation in clinical practice and
620 research. *Clin Neurophysiol* 120: 2008-2039, 2009.

621 **Royden CS, Banks MS, Crowell JA.** The perception of heading during eye movements.
622 *Nature* 360: 583–58, 1992.

623 **Saito H, Yukie M, Tanaka K, Hikosaka K, Fukada Y, Iwai, E.** Integration of direction
624 signals of image motion in the superior temporal sulcus of the macaque monkey. *J Neurosci*
625 6: 145-157, 1986.

626 **Schaafsma SJ, Duysens J.** Neurons in the ventral intraparietal area of awake macaque
627 monkey closely resemble neurons in the dorsal part of the medial superior temporal area in
628 their responses to optic flow patterns. *J Neurophysiol* 76: 4056–68, 1996.

629 **Seiffert AE, Somers DC, Dale AM, Tootell RBH.** Functional MRI studies of human visual
630 motion perception: texture, luminance, attention and after-effects. *Cereb Cortex* 13: 340-349,
631 2003.

632 **Sereno MI, Dale AM, Reppas JB, Kwong KK, Belliveau JW, Brady TJ, Rosen BR,**
633 **Tootell, RB.** Borders of multiple human visual areas in humans revealed by functional MRI.
634 *Science* 268:889-893, 1995.

635 **Shipp S, Blanton M, Zeki S.** A visuo-somatomotor pathway through superior parietal cortex
636 in the macaque monkey: cortical connections of areas V6 and V6A. *Eur J Neurosci* 10:3171-
637 3193, 1998.

638 **Silson EH, McKeefry DJ, Rodgers J, Gouws AD, Hymers M, Morland AB.** Specialized
639 and independent processing of orientation and shape in visual field maps LO1 and LO2. *Nat*
640 *Neurosci* 16:267-269, 2013.

641 **Smith AT, Wall MB, Williams AL, Singh KD.** Sensitivity to optic flow in human cortical areas
642 MT and MST. *Eur J Neurosci* 23: 561-569, 2006.

643 **Smith AT, Greenlee MW, Singh KD, Kraemer FM, Hennig J.** The processing of first- and
644 second-order motion in human visual cortex assessed by functional magnetic resonance
645 imaging (fMRI). *J Neurosci* 18: 3816–3830, 1998.

646 **Strong SL, Silson EH, Gouws AD, Morland AB, McKeefry, DJ.** A Direct Demonstration of
647 Functional Differences between Subdivisions of Human V5/MT+. *Cereb Cortex* doi:
648 10.1093/cercor/bhw362, 2016.

649 **Tanaka K, Saito H.** Analysis of motion of the visual field by direction, expansion /
650 contraction, and rotation cells clustered in the dorsal part of the medial superior temporal
651 area of the macaque monkey. *J Neurophysiol* 62: 626–641, 1989.

652 **Tanaka K, Fukada Y, Saito H.** Underlying mechanisms of the response specificity of the
653 expansion/contraction and rotation cells in the dorsal part of the medial superior temporal
654 area of the macaque monkey. *J Neurophysiol* 62: 642–656, 1989.

655 **Tootell RBH, Reppas JB, Kwong KK, Malach R, Born IT, Brady TJ, Rosen BR,**
656 **Belliveau JW.** Functional analysis of human MT and related visual cortical areas using
657 magnetic resonance imaging. *J Neurosci* 15: 3215-3230, 1995.

658 **Tootell RBH, Mendola JD, Hadjikhani NK, Ledden PJ, Liu AK, Reppas JB, Sereno MI,**
659 **Dale AM.** Functional analysis of V3A and related areas in human visual cortex. *J Neurosci*
660 17: 7060-7078, 1997.

661 **Tsao DY, Vanduffel W, Sasaki Y, Fize D, Knutsen TA, Mandeville JB, Wald LL, Dale AM,**
662 **Rosen BR, Van Essen DC, Livingstone MS, Orban GA, Tootell RBH.** Stereopsis activates
663 V3A and caudal intraparietal areas in macaques and humans. *Neuron* 39: 555-568, 2003.

664 **Vanduffel W, Fize D, Peuskens H, Denys K, Sunaert S, Todd JT, Orban GA.** Extracting
665 3D from motion: differences in human and monkey intraparietal cortex. *Science* 298: 413-
666 415, 2002.

667 **Wandell BA, Dumoulin SO, Brewer AA.** Visual field maps in human cortex. *Neuron* 56:366-
668 383, 2007.

669 **Warren WH, Hannon DJ.** Direction of self-motion is perceived from optical flow. *Nature* 336:
670 162-163, 1988.

671 **Warren PA, Rushton SK.** Optic flow processing for the assessment of object movement
672 during ego movement. *Curr Biol* 19: 1555-1560, 2009.

673 **Wassermann EM.** Risk and safety of repetitive transcranial magnetic stimulation: report and
674 suggested guidelines from the International Workshop on the Safety of Repetitive
675 Transcranial Magnetic Stimulation. *Electroenceph Clin Neurophysiol* 108: 1-16, 1998.

676 **Watson JD, Myers R, Frackowiak RS, Hajnal JV, Woods RP, Mazziotta JC, Shipp S,
677 Zeki S.** Area V5 of the human brain: evidence from a combined study using positron
678 emission tomography and magnetic resonance imaging. *Cereb Cortex* 3: 79-94, 1993.

679 **Wall MB, Smith AT.** The representation of egomotion in the human brain. *Curr Biol* 18:191-
680 194, 2008.

681 **Wall MB, Lingnau A, Ashida H, Smith AT.** Selective visual responses to expansion and
682 rotation in the human MT complex revealed by functional magnetic resonance imaging
683 adaptation. *Eur J Neurosci* 27: 2747-2757, 2008.

684 **Yu X, Hou H, Spillmann L, Gu Y.** Causal evidence of motion signals in macaque middle
685 temporal area weighted-pooled for global heading perception. *Cereb Cortex* doi:
686 10.1093/cercor/bhw402, 2017.

687 **Zeki S, Watson JDG, Lueck CJ, Friston KJ, Kennard C, Frackowiak RSJ.** A direct
688 demonstration of functional specialization in the human visual cortex. *J Neurosci* 11:641-
689 649, 1991.

690 **Zhang T, Britten KH.** The responses of VIP neurons are sufficiently sensitive to support
691 heading judgments. *J Neurophysiol* 103:1865-1873, 2010.

692 **Zhang T, Britten KH.** Parietal area VIP causally influences heading perception during
693 pursuit eye movements. *J Neurosci* 31:2569-2575, 2011.

694

695

696

697

698

699

700

701

702

703

704

705 **Tables**

		x	y	z
MST/TO-2	<i>This Study (n=7)</i>	42 ± 5	-69 ± 9	0 ± 9
	<i>Dukelow et al., 2001 (n=8)</i>	45 ± 3	-60 ± 5	5 ± 4
	<i>Kolster et al., 2010 (n=11)</i>	44	-70	5
V3A	<i>This Study (n=7)</i>	17 ± 6	-93 ± 5	15 ± 8
	<i>Tootell et al., 1997 (n=5)</i>	29	-86	19
LO-1	<i>This Study (n=7)</i>	27 ± 6	-89 ± 2	1 ± 3
	<i>Larsson and Heeger, 2006 (n=15)</i>	32 ± 4	-89 ± 5	3 ± 7

706

707 **Table 1.** Average Talairach co-ordinates for centre of target TMS sites (MST/TO-2, V3A, LO-1) in right
 708 hemisphere (RH) ± standard deviation (where available). Results from the current study are compared
 709 with previous data as cited in the table.

710

711

712

713

714

	Mean	Std. Deviation
Experiment 1 (Radial)		
Percent Correct (%)	76.86	8.15
Response Times (s)	0.73	0.28
Experiment 2 (FOE)		
Percent Correct (%)	73.25	7.32
Response Times (s)	0.65	0.20

715

716 **Table 2.** Means and standard deviations for percent correct and response times for the
 717 correlational analysis.

718

719 **Figure Legends**

720 **Figure 1.** *TMS/Behavioural Paradigms. Experiment 1: radial motion stimuli (expanding or contracting)*
721 *were presented in a circular aperture displaced 15° to the left of a fixation cross. The onset of a*
722 *repetitive train of 5 TMS pulses was coincident and coextensive with the onset of this stimulus.*
723 *Following stimulus offset the participants reported the perceived direction of the motion (in or out) by a*
724 *key press. Experiment 2: each test sequence began with the onset of a reference stimulus (200 ms)*
725 *comprising a circular aperture of radially expanding dots embedded in a background of randomly*
726 *moving noise dots. After a 2000 ms delay a test stimulus was presented, in which the FOE of the*
727 *radial motion was displaced either upwards or downwards. The delivery of the TMS pulse train was*
728 *coincident with the onset of the test stimulus. Following test offset participants reported the perceived*
729 *direction of FOE displacement (up or down) by a key press.*

730

731 **Figure 2.** *Location of main cortical ROI target sites for TMS. Inflated right hemispheres for two*
732 *subjects (S3 and S7) with overlaid positions of TMS target sites used in experiment 1 and experiment*
733 *2. The bottom figure shows a magnified view of the posterior section of the hemisphere. The*
734 *representation of the visual field in each area is denoted with a symbol ('+' / '-'). A '+' indicates*
735 *representation of the superior contra-lateral visual field; whilst '-' indicates the inferior contra-lateral*
736 *visual field. These markings are absent from the representations of MST/TO-2 as the retinotopic*
737 *mapping did not produce reliable maps within these regions.*

738

739 **Figure 3.** *Average Percent Correct Data from Experiment 1 and Experiment 2. Bar charts showing*
740 *average percent correct (%) across experiment 1 (a) and experiment 2 (b). Error bars represent*
741 *S.E.M. Asterisks represent significance at $p < 0.05$ (*) and $p < 0.01$ (**).*

742

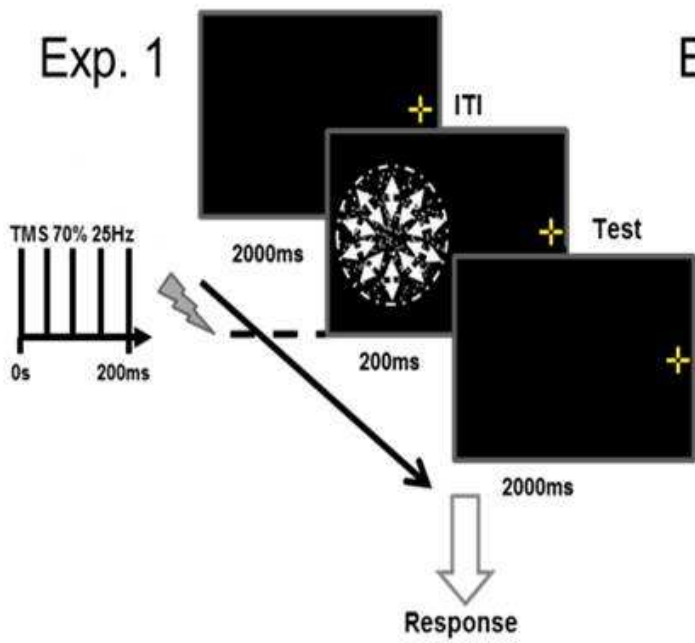
743 **Figure 4.** *Average Response Time Data from Experiment 1 and Experiment 2. Bar charts showing*
744 *average response time (s) across experiment 1 (a) and experiment 2 (b). Error bars represent S.E.M.*

745

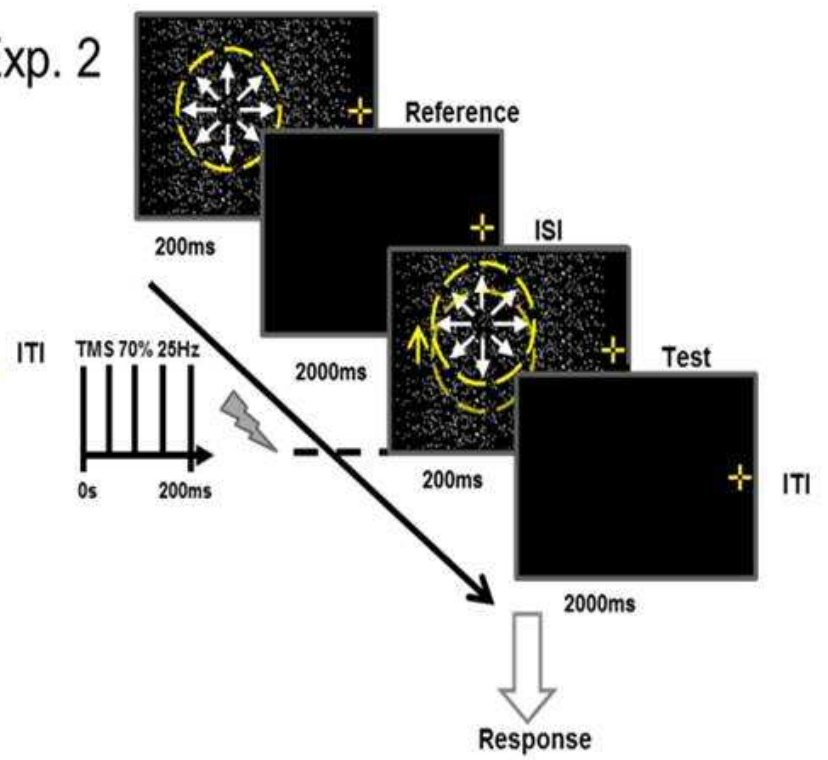
746 **Figure 5.** *Correlational Data for Percent Correct and Response Time from Experiment 1 and*
747 *Experiment 2. A scatter plot showing relationship between percent correct and response time across*
748 *experiment 1 (Radial) and experiment 2 (FOE). Error bars represent S.E.M. Asterisks represent*
749 *significance at $p < 0.05$ (*).*

750

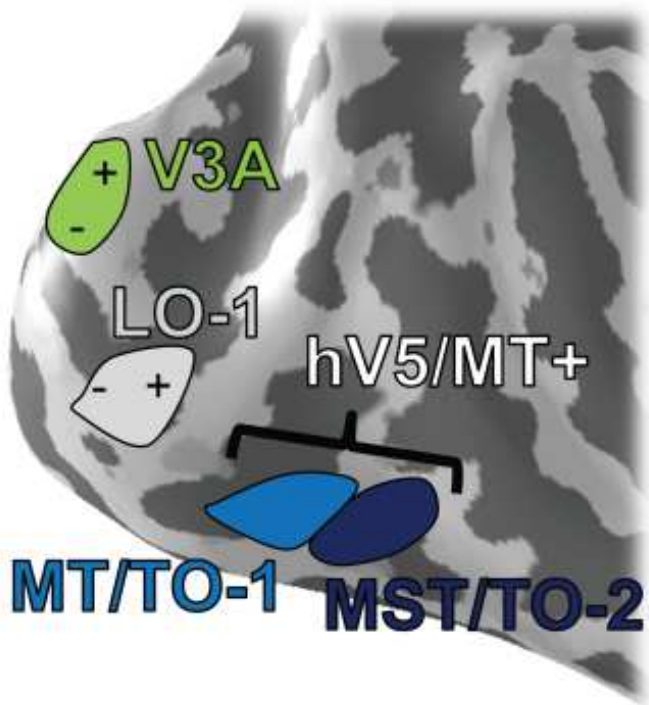
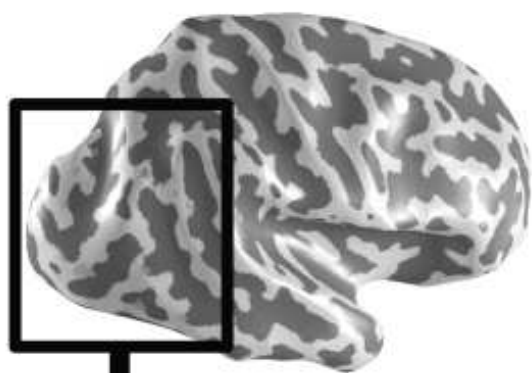
Exp. 1



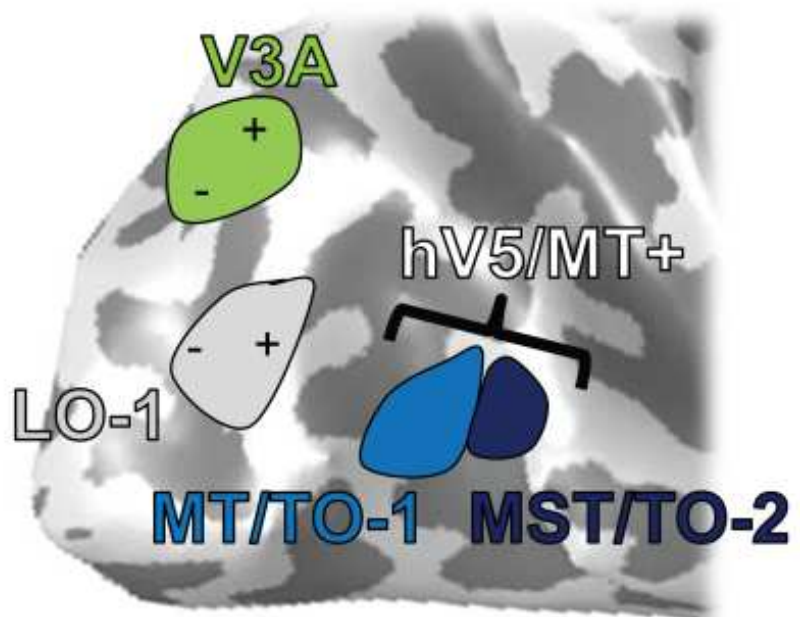
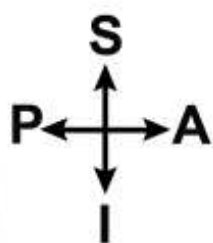
Exp. 2

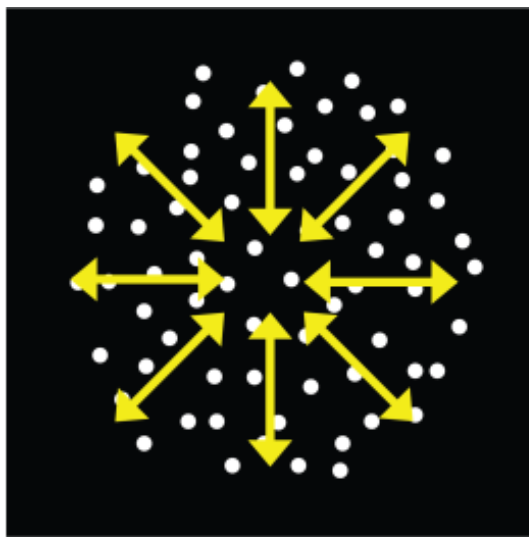


S3

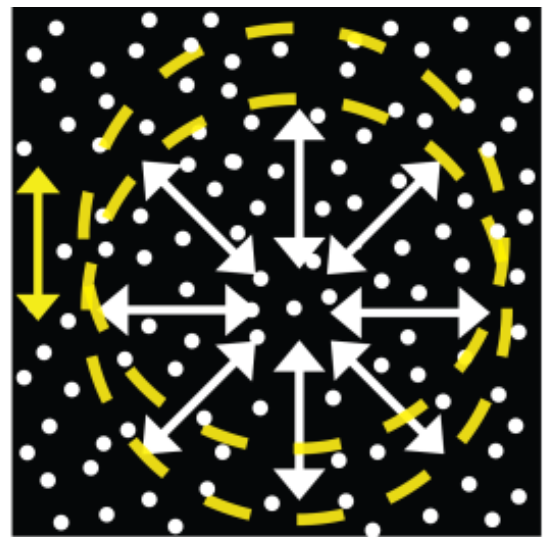


S7

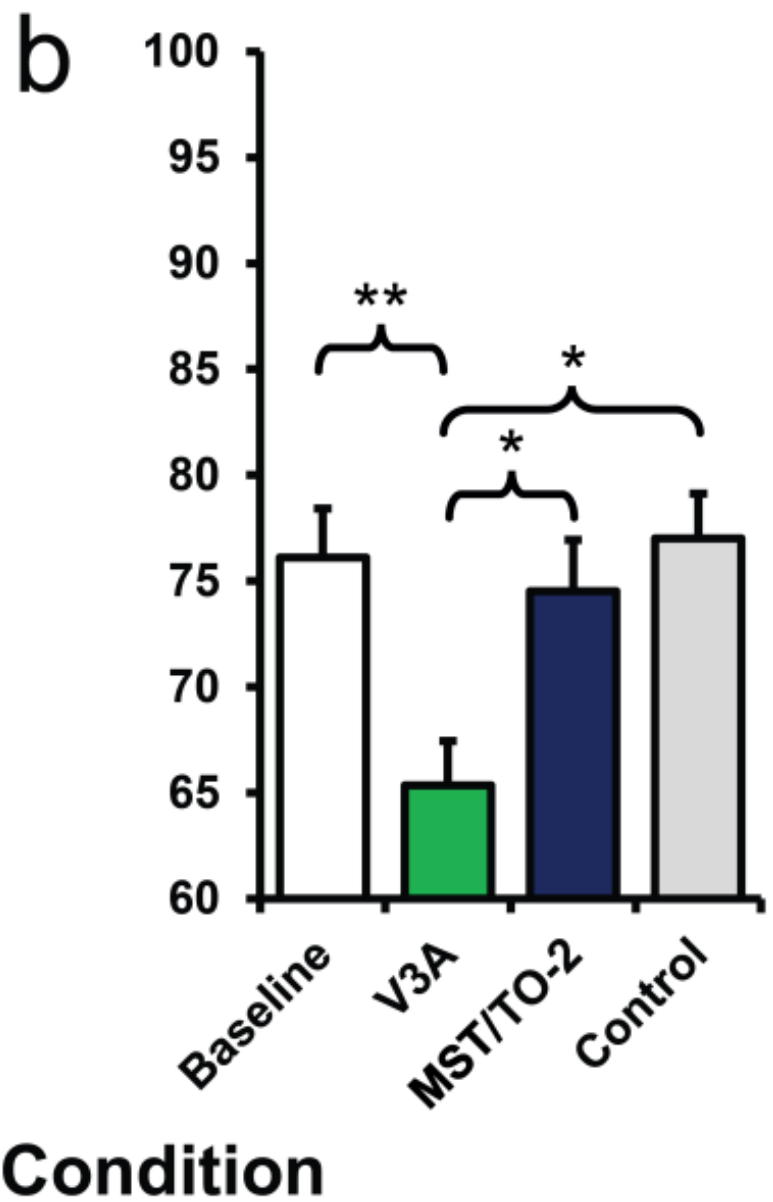
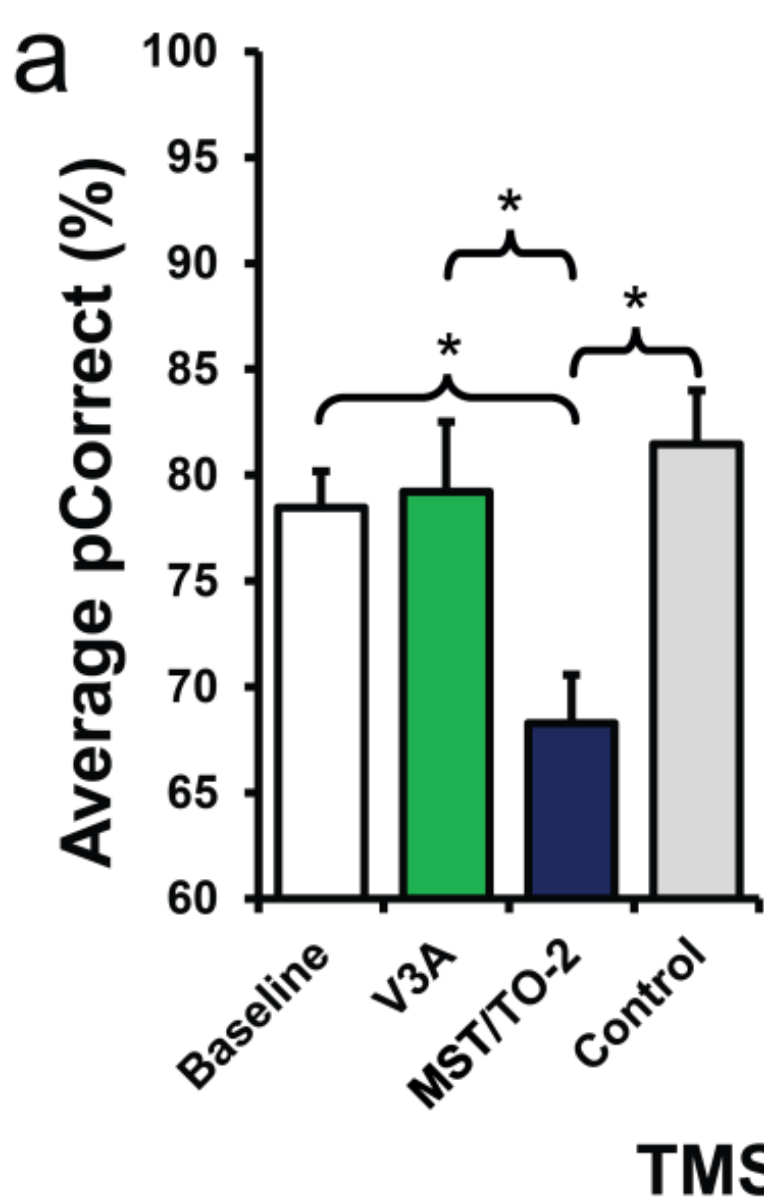


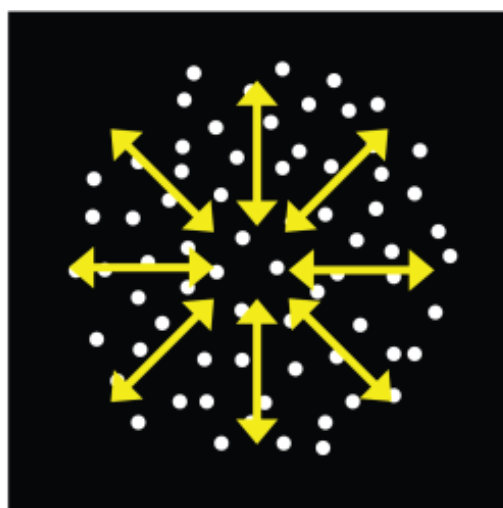


Exp. 1 - Radial

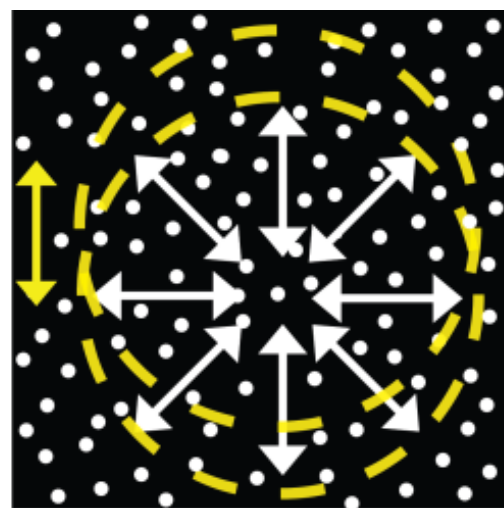


Exp. 2 - FOE

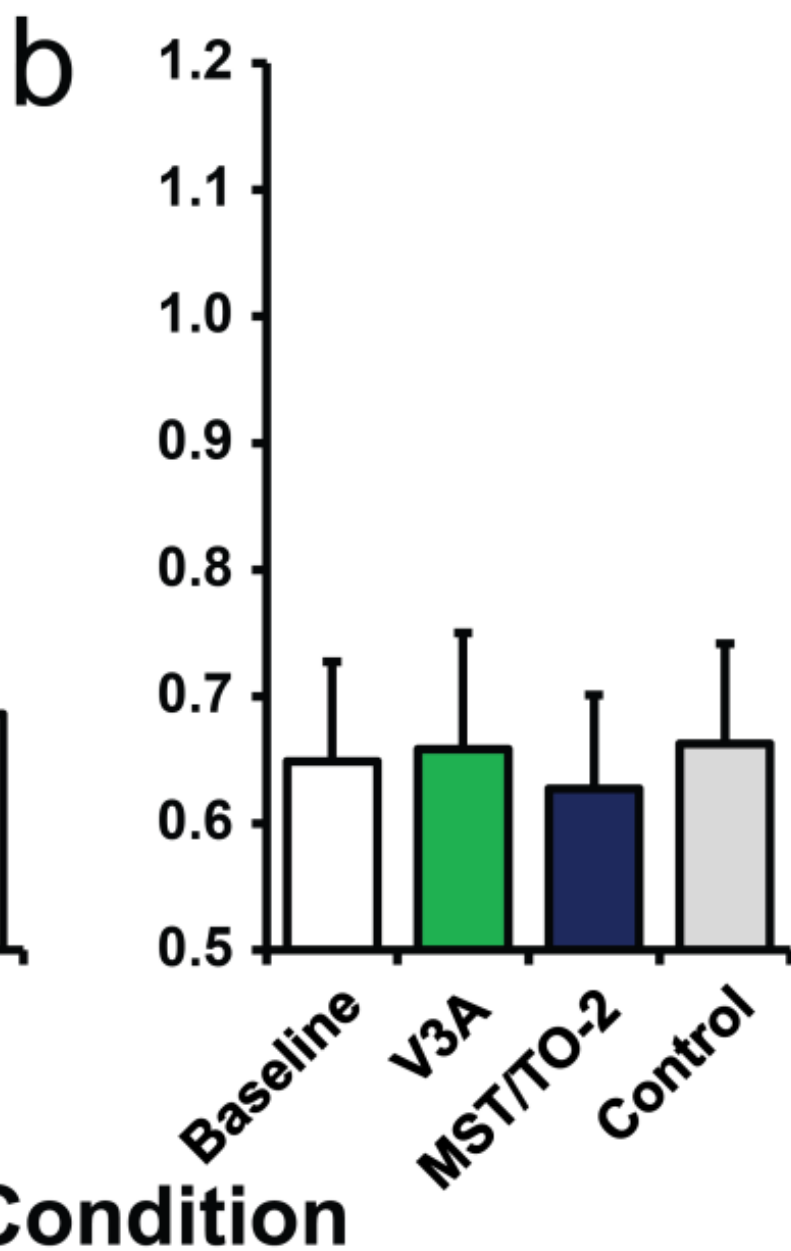
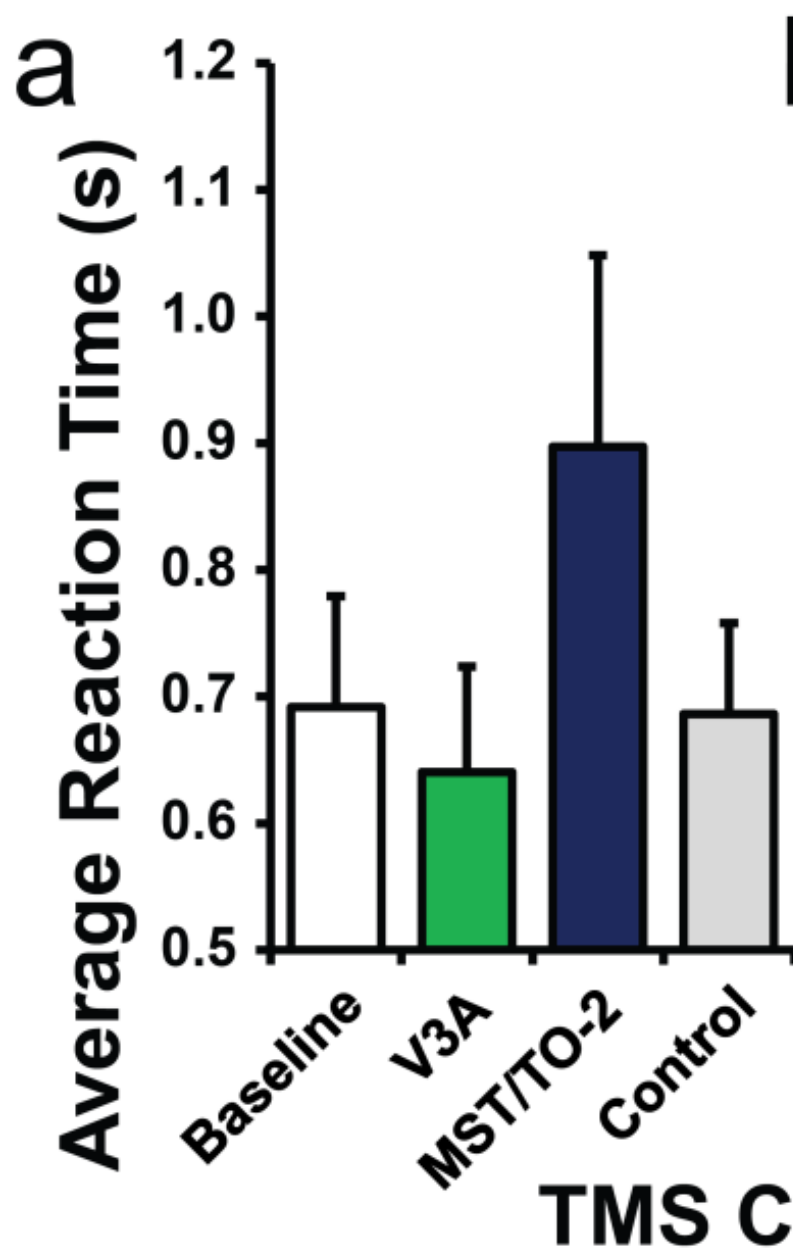


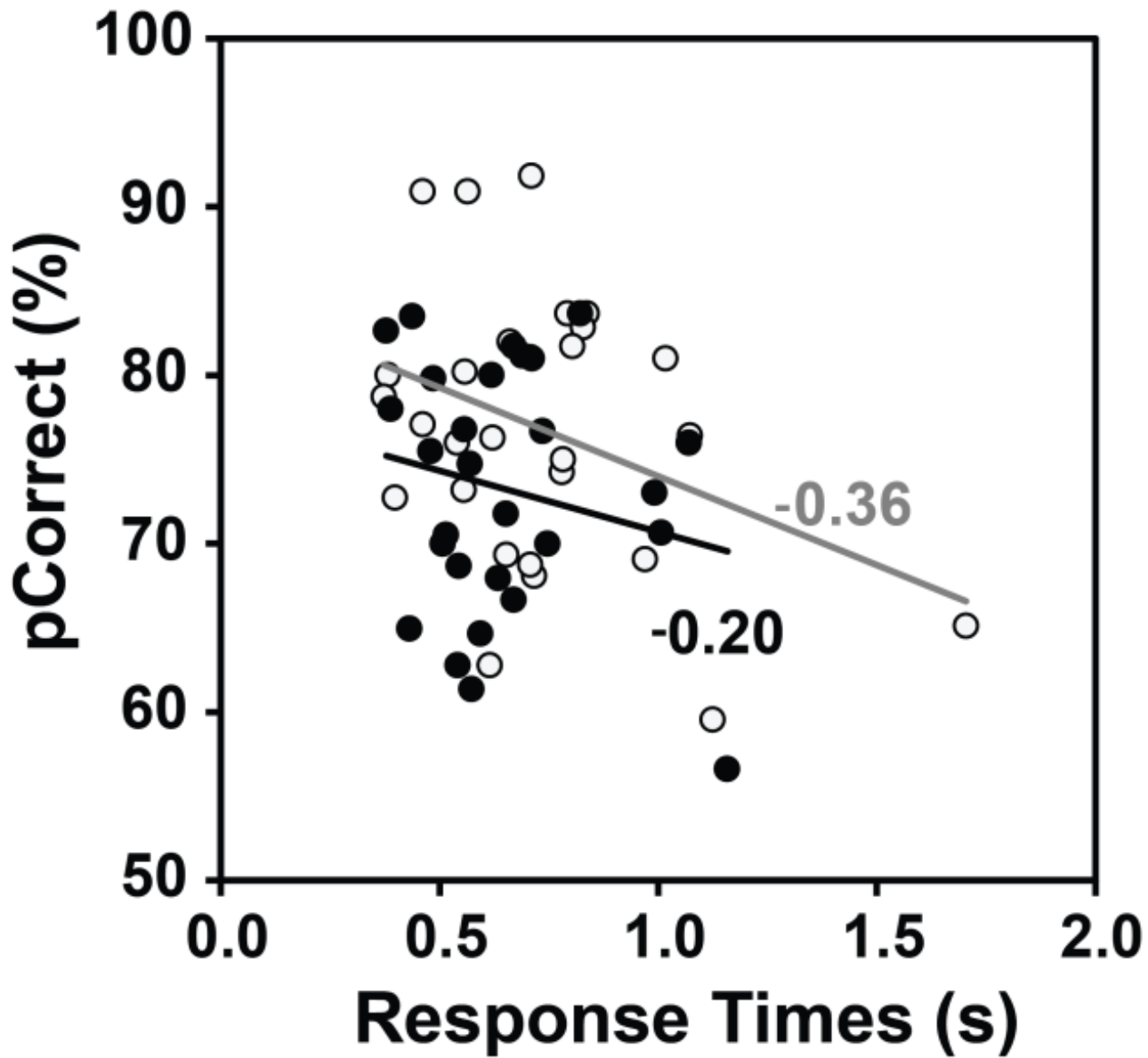


Exp. 1 - Radial



Exp. 2 - FOE





- Exp. 1 - Radial
- Exp. 2 - FOE